Physics of the Earth and Planetary Interiors 276 (2018) 86–92

Contents lists available at ScienceDirect

Physics of the Earth and Planetary Interiors

journal homepage: www.elsevier.com/locate/pepi

Crystallization of a compositionally stratified basal magma ocean

Matthieu Laneuville [a,*], John Hernlund [a], Stéphane Labrosse [b], Nicholas Guttenberg [a]

[a] Earth-Life Science Institute, Tokyo Institute of Technology, 2-12-IE-1 Ookayama, Meguro-ku, Tokyo 152-8551, Japan
[b] Laboratoire de géologie de Lyon, Université de Lyon, École normale supérieure de Lyon, Université Lyon-1, CNRS, UMR 5276, F-69364 Lyon, France

ARTICLE INFO

Article history:
Received 15 February 2017
Received in revised form 14 June 2017
Accepted 24 July 2017
Available online 29 July 2017

Keywords:
Earth
Magma ocean
Geodynamo

ABSTRACT

Earth's ~3.45 billion year old magnetic field is regenerated by dynamo action in its convecting liquid metal outer core. However, convection induces an isentropic thermal gradient which, coupled with a high core thermal conductivity, results in rapid conducted heat loss. In the absence of implausibly high radioactivity or alternate sources of motion to drive the geodynamo, the Earth's early core had to be significantly hotter than the melting point of the lower mantle. While the existence of a dense convecting basal magma ocean (BMO) has been proposed to account for high early core temperatures, the requisite physical and chemical properties for a BMO remain controversial. Here we relax the assumption of a well-mixed convecting BMO and instead consider a BMO that is initially gravitationally stratified owing to processes such as mixing between metals and silicates at high temperatures in the core-mantle boundary region during Earth's accretion. Using coupled models of crystallization and heat transfer through a stratified BMO, we show that very high temperatures could have been trapped inside the early core, sequestering enough heat energy to run an ancient geodynamo on cooling power alone.

1. Introduction

Conducted heat loss is thought to be one of the greatest hurdles for a terrestrial planet to overcome in the long-term sustenance of a magnetic field by dynamo action (Stevenson, 2003). To avoid thermal stratification and cessation of convection currents that sustain the dynamo, this conducted heat must either be taken up into the overlying sluggishly convecting solid mantle or returned into the deeper core under the influence of a stronger buoyancy source (Badro et al., 2016; O'Rourke et al., 2017; O'Rourke and Stevenson, 2016; Hirose et al., 2017) or strong mechanical stirring (Cébron et al., 2010; Le Bars et al., 2015). Heat loss to the mantle results in core cooling, while re-ingestion of conducted heat can partly delay core cooling. While crystallization of Earth's solid inner core may provide a significant composition-induced buoyancy source for re-ingesting heat at the present day, the inner core itself has likely existed for only a fraction of the age of the geomagnetic field. Unless there is another buoyancy source to help drive convection prior to inner core crystallization (O'Rourke and Stevenson, 2016; Badro et al., 2016; O'Rourke et al., 2017; Hirose et al., 2017), heat loss from the core to the mantle implies a minimum of 500–1000 K of core cooling since 3.5 Ga (Gomi et al., 2013; Labrosse, 2015). The actual cooling would be significantly higher if one accounted for fluctuations in heat flow. The ~7–14 TW of core-mantle boundary (CMB) heat flow that is compatible with recent estimates (Lay et al., 2008; Hernlund and McNamara, 2014) may be insufficient to account for this degree of secular cooling.

Recent estimates of Earth's core conductivity are roughly twice to thrice as high as some earlier estimates (de Koker et al., 2012; Pozzo et al., 2012; Gomi et al., 2013), which contributes to the high degree of estimated core cooling. The precise value of the core conductivity is still highly debated but studies performed before that debate and using values of conductivity in the lower end of the current debate or even smaller already recognized that the requisite core cooling prior to the birth of the inner core meant that the ancient core-mantle boundary (CMB) may have been hotter than the solidus temperature of rocks in the deep mantle (Buffett, 2002; Labrosse et al., 2007). Combined with observations of ultra-low velocity zones at the bottom of the mantle that have often been ascribed to the presence of partial melt (e.g. Williams and Garnero, 1996; Labrosse et al., 2015), even modest cooling rates of the core imply a larger amount of melt in the past, leading to the idea of an extensive "basal magma ocean" (BMO) of up to ~1000 km thickness that may have existed at the bottom of the early Earth's mantle (Labrosse et al., 2007).

Earlier models of BMO evolution were relatively simplistic, utilizing an idealized phase diagram and assuming a homogeneous magma existed at the end of Earth's accretion. However, accretion itself was probably a messy process, and is unlikely to have pro-

* Corresponding author.
E-mail address: mlaneuville@elsi.jp (M. Laneuville).

http://dx.doi.org/10.1016/j.pepi.2017.07.007
0031-9201/

duced the kind of neat conditions we have assumed in past models. It is therefore worth relaxing previous assumptions to explore whether the evolution model can permit a wider range of core secular cooling histories.

Here we consider the possibility that a dense iron-rich silicate melt could have formed in the core-mantle boundary region of the early Earth via silicate-metal mixing between liquids at high temperatures, for example following a giant impact event. During silicate-metal mixing, we expect a chemical reaction of the following kind:

$$SiO_2^{Sil} + 2Fe^{Met} \rightarrow Si^{Met} + 2FeO^{Met+Sil}. \quad (1)$$

The superscripts Sil and Met denote the silicate and metal liquids, respectively. Higher temperatures are known to shift reactions of this kind to the right (Tsuno et al., 2013; Fischer et al., 2016; Hernlund, 2016). Dissolution of Si from an oxide state into metal at higher temperature is accompanied by production of FeO, some of which may remain in solution in metallic liquid and some of which will be partitioned into the silicate liquid. Fig. 1 illustrates the evolution scenarios considered in previous models compared to the present study.

There are many possible scenarios in which FeO-enriched melts can be produced by silicate-metal mixing at high temperatures in the CMB region. For example, in a scenario where the Moon is formed by a giant impact between a Mars-sized embryo and the proto-Earth (e.g. Canup, 2004; Canup, 2012), extensive turbulent mixing should occur between the in-falling impactor core and the surrounding molten mantle silicates (Deguen et al., 2014). The resultant heavy silicate-metal mixture would be expected to sink to the CMB region, after which metal droplets would separate from the silicate liquid onto the top of the core. Such a process would leave behind a FeO-rich silicate liquid at the bottom of the mantle, and produce a Si- and O-enriched metallic fluid atop the core. Such structures in the core could remain even after crystallization of the molten mantle, so long as they are stable against turbulent entrainment (Landeau et al., 2016). Such a mechanism may be compatible with layering observed by seismological analysis of the shallow core (Helffrich and Kaneshima, 2010).

Production of FeO-rich fluid at the base of the mantle changes two key properties that permit such a liquid to persist long after Earth's formation. The first is a density increase, allowing the FeO-rich melt to remain gravity-stabilized beneath the overlying relatively FeO-poor mantle. The second is a depression in the freezing temperature (i.e., liquidus) which can allow the melt to persist after the overlying mantle has solidified. The latter property occurs because FeO is slightly (Andrault et al., 2011) to moderately (Nomura et al., 2011; Tateno et al., 2014) incompatible and hence promotes melting. This mechanism for producing a BMO is distinct from previously discussed scenarios involving mid-mantle crystallization from a homogeneous molten mantle at the intersection of the liquid isentrope and liquidus, overturning and remelting of a fractionally crystallized solid mantle, or melting from below of the mantle owing to the initial superheat in the core (Labrosse et al., 2015). The efficacy of this mechanism for initially producing a BMO also does not depend upon the density difference between melt and solid in equilibrium, although such difference would still lead to different evolutionary scenarios.

The silicate-metal mixing scenario is unlikely to produce a homogeneous well-mixed fluid underlying a relatively iron-poor mantle. Owing to variable degrees of chemical interaction, heterogeneous temperature, and partial mixing between the dense liquid and overlying mantle, it is more natural to expect a gradient in density inside the residual silicate liquid, characterized by increasing FeO-content with depth inside the layer. Such a layer would not convect unless the thermal gradient were sufficiently steep to overcome the stratifying effects of FeO.

The goal of this paper is to test the influence of an initially stratified, liquid silicate layer at the core mantle boundary on the thermal evolution of the core. We chose to approach the problem from a parametric perspective, to characterize the importance of a range of parameters on observables. Therefore this model cannot be used to predict the degree of stratification or the size of the layer, but rather provide tools to understand how such a layer would fit in a global view of the early evolution of the Earth.

In the following, we first present equations to compute the erosion of the stratification as the layer crystallizes. We then provide a description of its implementation in an evolution simulation and a discussion of the choice of parameters. In the results section, we first describe the erosion process, irrespective of any particular evolution scenario. Only after do we present typical predicted evolution and discuss its influence on core cooling.

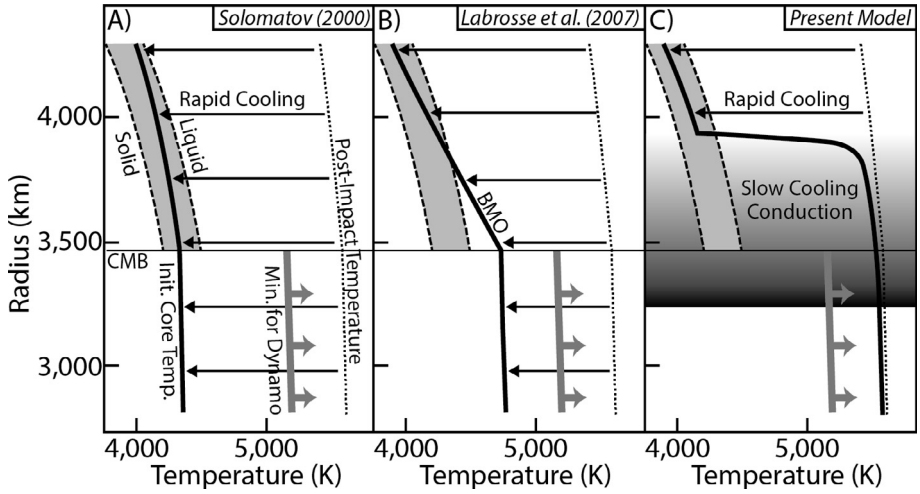

Fig. 1. Illustration of evolution scenarios considered in previous models, compared to the present model. The classic scenario (A) is one where the magma ocean isentrope is less steep than the liquidus, and the mantle freezes from the bottom-up. The generic BMO scenario (B) involves a magma ocean isentrope steeper than the liquidus, such that freezing begins at depths shallower than the CMB and trapping a basalt melt below. In the present case (C), the magma ocean rapidly cools to the liquidus above a layer gravitationally stratified by enrichment in FeO, but cooling of the layer and the underlying core is inhibited by sluggish heat conduction through the stratified layer. In scenarios A and B the initial core temperature is too low to allow for the large secular core cooling that is required in order for thermal convection to power the dynamo for billions of years with a relatively large core thermal conductivity.

2. Model

We now consider the evolution of the initially stably stratified liquid silicate layer. The tendency for such a stratified BMO to crystallize from the top is enhanced owing to relative depletion of FeO with height. Fractional crystallization (with solids containing relatively lower concentrations of FeO) leaves behind a magma that is enriched in FeO compared to its initial composition. This triggers compositional convection that erodes the underlying stratification.

We separate the problem into a time-independent part, describing the erosion of the stratification through mass balance uniquely for different degrees of arbitrary crystallization. We then embed this into a complete thermal evolution coupling the overlying mantle and underlying core to describe the time evolution.

2.1. Erosion of the stratification

Upon crystallization, the top of the stratified layer becomes increasingly enriched in dense iron. As the fraction of FeO in the topmost liquid increases, its FeO content eventually exceeds that of the underlying fluids immediately below. This causes a Rayleigh–Taylor unstable situation that leads to overturn, mixing, and erosion of the layer stratification driven from above. Using mass balance arguments and assuming a well mixed convective region forms at the top of the BMO as this erosion proceeds, it is possible to track composition changes between the different reservoirs and compute how much of the profile will be eroded by incremental crystallization at the top of the layer. Fig. 2 illustrates some of the notations used in the following sections.

The mass balance for component i in the convective layer can conveniently be written as

$$\delta(mc) = \delta m_{top}(c + \Delta c^{l/s}) + \delta m_{bot}(c + \Delta c^{str}), \tag{2}$$

where m is the mass of the convective layer and c its concentration in component i. Increments δm_{top} and δm_{bot} are mass changes due to crystallization at the upper boundary (net sink, $\delta m_{top} < 0$), and erosion of the stratification at the lower boundary (net source, $\delta m^{bot} > 0$), respectively. The parameter $\Delta c^{l/s}$ is the composition difference between liquid and solid at the top, and Δc^{str} between the convecting and neighboring stratified liquid at the bottom interface. The very top of the stratified region has the same composition as the convecting liquid, but with downward erosion has an excess composition, which can be considered negligible to first order. Eq. (2) can then be rewritten as

$$m\delta c = -c(\delta m + \delta m_{top} + \delta m_{bot}) + \Delta c^{l/s}\delta m_{top} \tag{3}$$

where the first term on the right hand side is exactly zero. Rewriting mass changes as radius changes and using b and t subscript for bottom and top radius, respectively, a differential equation for the composition can then be obtained

$$\frac{dc}{dr_t} = \frac{3r_t^2\Delta c^{l/s}}{r_t^3 - r_b^3}. \tag{4}$$

To solve for the crystallization front position r_t that is required in order to have a convective zone that extends down to the bottom radius r_b, one finally needs to define the strength of the stratification gradient dc/dr = γ. Replacing composition in Eq. (4) then leads to

$$\frac{dr_b}{dr_t} = \frac{3r_t^2}{r_t^3 - r_b^3}\frac{\Delta c^{l/s}}{\gamma}, \tag{5}$$

which can be solved to obtain

$$r_t^3 = 6B^3\left(1 - e^{-\frac{R-r_b}{B}}\right) + 6B^2\left(r_b - Re^{-\frac{R-r_b}{B}}\right) + 3B\left(r_b^2 - R^2e^{-\frac{R-r_b}{B}}\right) + r_b^3, \tag{6}$$

where R is the initial radius of the top of the basal magma ocean, and $B = \Delta c^{l/s}/\gamma$. The time required to crystallize down to this radius however depends on the energy balance of the magma layer, which we compute independently.

2.2. Thermal evolution

The previous considerations were time independent, considering the effect of an arbitrary crystallization increment on the underlying structure. To assess the timing of evolution, we now use a 1D heat conduction model, where convection is included through an effective conductivity (Sasaki and Nakazawa, 1986; Kimura et al., 2009)

$$\frac{\partial Q}{\partial t} = \frac{1}{r^2}\frac{\partial}{\partial r}\left(kr^2\frac{\partial T}{\partial r}\right) + \frac{1}{r^2}\frac{\partial}{\partial r}\left(r^2F_{conv}\right) + \rho H, \tag{7}$$

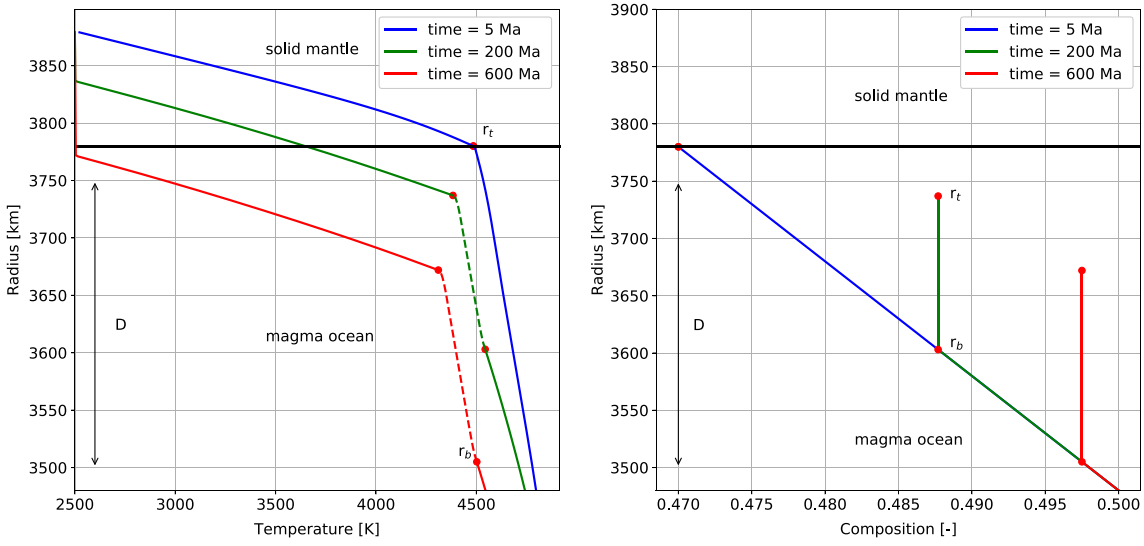

Fig. 2. Example evolution of (top) temperature profiles and (bottom) composition to illustrate notations. D is the initial thickness of the molten layer, r_b and r_t are the bottom and top of the convective zone, respectively. This figure shows how the convective zone (dashed lines) grows as the layer crystallizes, steepening the thermal gradient of the stratified zone in the process. In the bottom panel, composition is uniform within the convective region, and retains its initial stratification below.

where Q is the heat content in Jm^{-3}, t is time, r is radius, T is temperature, k is thermal conductivity, H is radioactive heating, and F_{conv} is the effective convected heat flow. Eq. (7) is then solved from the core mantle boundary to 100 km above the initial magma ocean upper boundary. The boundary condition is a constant 2500 K at the top, and the core is a cooling heat bath with initial temperature T_{core}. Following Sasaki and Nakazawa (1986) and Kimura et al. (2009) we consider a parametrization of convective heat flow based on mixing length theory (e.g., Spiegel, 1963). The convective heat flow is computed as

$$F_{conv} = \begin{cases} \frac{\rho c_p \alpha g l^4}{18\nu} \left[\left(\frac{dT}{dr}\right)_s - \frac{dT}{dr}\right]^2, & \left[\left(\frac{dT}{dr}\right)_s - \frac{dT}{dr}\right] > 0 \\ 0, & \left[\left(\frac{dT}{dr}\right)_s - \frac{dT}{dr}\right] \leqslant 0 \end{cases} \quad (8)$$

where ρ is density, c_p specific heat, α thermal expansivity, g gravitational acceleration, ν kinematic viscosity, l a characteristic length and the subscript s refers to the isentropic state. The characteristic length is chosen to be the distance to the closest boundary ($l(r) = \min(r_t - r,\ r - r_b)$, Kimura et al. (2009)). The adiabatic gradient is set to $\alpha g T/c_p$, with the parameters values from Table 1. Finally the temperature is obtained from the heat content Q as

$$T(Q) = \begin{cases} \frac{Q}{\rho c_p}, & Q - \rho c_p T_L < 0 \\ \frac{Q - Q_L}{\rho c_p}, & Q - \rho c_p T_L > Q_L \\ T_L, & \text{otherwise}, \end{cases} \quad (9)$$

where Q_L is the latent heat of crystallization and T_L the liquidus temperature.

The liquidus is a linear function of composition

$$T_L(c) = T_L^0 - (c - c_0)\Delta T_L \quad (10)$$

with $T_L^0 = 4500$ K, ΔT_L is the liquidus drop between the iron-rich and iron-poor end members and c_0 is the initial liquid composition. The idealized phase diagram is the same as that used in Labrosse et al. (2007). Assuming that solute diffusion is negligible in the stably stratified layer, the composition evolves only in the convective zone where it takes the value of its lower boundary.

2.3. Model parameters and initial conditions

The layer is initially setup with a linear composition profile, anchored so that the liquidus at the top of the layer is 4500 K. The radius independent composition gradient γ is a parameter of the models (we always quote its absolute value, but density is decreasing with radius). The initial radioactive heat sources content is assumed to be chondritic (McDonough and Sun, 1995). During crystallization, heat sources remain entirely in the liquid and therefore become more concentrated with time.

The initial temperature gradient follows a 1 K/km gradient and the core temperature is set to the value at the core mantle boundary. The solid mantle is considered as a heat bath at 2500 K, coupled to the basal magma ocean through a 100 km-thick conductive boundary layer with thermal diffusivity K_b. The mantle itself is given a high thermal diffusivity K_m to insure temperature remains constant and then evolves according to the diffusion equation.

Values for the fixed parameters can be found in Table 1.

Table 1
Values of the fixed parameters of the model.

Name	Variable	Value	Units
Core radius	R_c	3480	km
Average density	ρ	5000	kg m^{-3}
Latent heat	L	7.5 10^9	J m^{-3}
Thermal expansivity	α	2 10^{-5}	K^{-1}
Specific heat	c_p	1000	J kg^{-1} K^{-1}
Liquid diffusivity	K_b	10^{-5}	m^2 s^{-1}
TBL diffusivity	K_m	2 10^{-6}	m^2 s^{-1}
Density gradient	γ	6000	kg m^{-3} wt.%$^{-1}$
Partitioning coef.	$\Delta c^{l/s}$	0.088	–
CMB gravity acceleration	g	11	m s^{-2}
Liquidus drop	ΔT_L	2000	K

3. Results

The strength of the stratification controls the rate at which it can be eroded (Fig. 3, top). A small stratification will be easier to erode, which also means that a lower fraction of the basal magma ocean will need to be crystallized before full erosion (Fig. 3, bottom). On the other hand, a strong stratification is harder to erode. This leads to cases where the convective zone quickly reaches a maximum size at which the rate of crystallization is similar to that of erosion. For instance, for a stratification of 10^{-7} wt.% m^{-1} and an initial layer thickness of 500 km, the entire stratification is eroded after only about 100 km of crystallization. For a stratification of 3 10^{-7} wt.% m^{-1}, more than 300 km of crystallization is required before complete erosion.

Once the convective zone evolution as a function of crystallization radius is known, it is possible to estimate the size of the

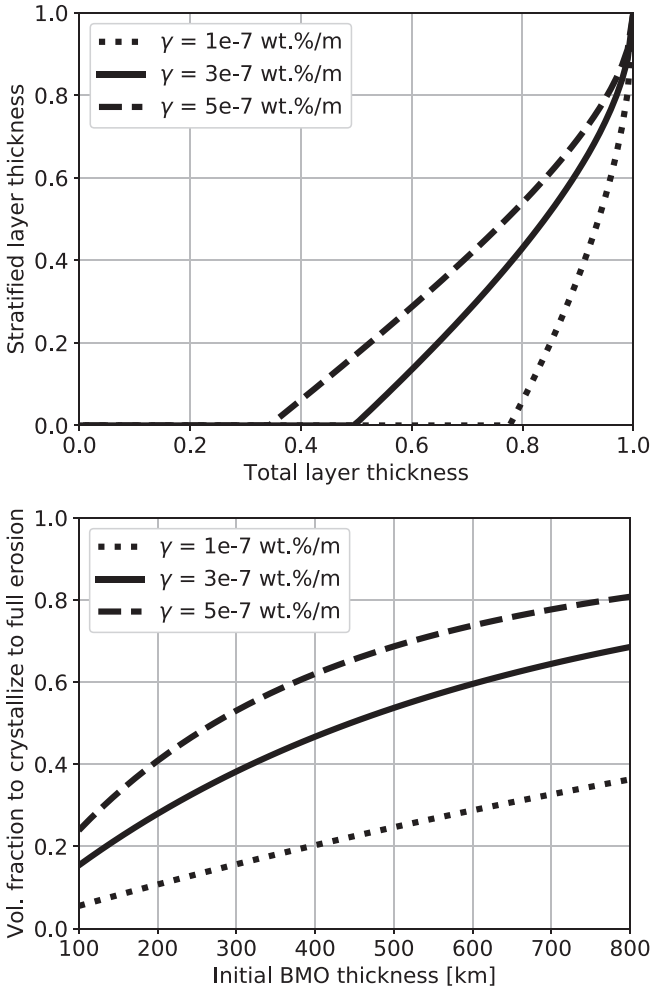

Fig. 3. (top) Growth of the convective zone for different composition gradients as a function of total layer thickness (for an initial BMO thickness D = 500 km), where thicknesses are normalized by the initial size of the layer. (bottom) Equivalent volume fraction to crystallize before complete erosion for the same set of composition gradients.

energy buffer that this layer represents. Fig. 4 (top) shows the total energy that needs to be extracted by the mantle to account for the latent heat of crystallization of the layer, the additional cooling required by the liquidus depression and the gravitational energy required to mix the initial stratification to a uniform concentration. This is shown as a function of D, the initial BMO thickness.

The total energy increases both with the size of the layer, and the strength of stratification. The values obtained are comparable to global core cooling of about 100–600 K, neglecting any contribution from inner core crystallization. For thin layers, the latent heat effect dominates, whereas at larger values gravitational energy required to mix the initial stratification dominates (Fig. 4, bottom). Fig. 4 (bottom) also shows the range of contributions over the range of compositional gradients. For small stratification for example the latent heat effect dominates, even for large initial BMO thicknesses.

Thermal evolution models using the analytical constraints on convection zone evolution and the energy balance of Eq. (7) show the influence of the layer on the core-mantle boundary heat flow. Fig. 5 shows the core mantle boundary heat flow evolution for several initial layer thicknesses D and composition gradients γ.

The general structure of the evolution has two peaks. The first one corresponds to the peak induced by erosion of the stratification, which actually steepens the temperature gradient of the stratified region (see Fig. 2). Compared to a well-mixed magma ocean this is a much smaller volume and it is therefore allowed to cool faster, leading to an efficient way of increasing the temperature difference between the convective zone and the core and thus, the heat flow.

Once erosion is complete, the temperature difference between the core and magma ocean goes to another "equilibrium" and the heat flow drops suddenly. Over time it reaches a second peak due to thinning of the magma ocean, as already observed in Labrosse et al. (2007). These features remain valid throughout the considered thickness and composition gradient range, only the timing and amplitude vary.

For a given compositional stratification, a larger layer reduces the average core mantle boundary heat flow (Fig. 6, top). This also changes the timing required to reach a certain core mantle boundary heat flow value and the time required for complete erosion. Fig. 6 (bottom) shows the dependence of this initial evolution on initial thickness and composition gradient. For thicknesses larger than that depicted in the figure, that threshold is never reached. Interestingly, while the composition gradient changes the timing of the peaks, it does not really influence the average core-mantle boundary heat flow value. This can be understood by the fact that a larger compositional gradient merely delays core cooling (as can

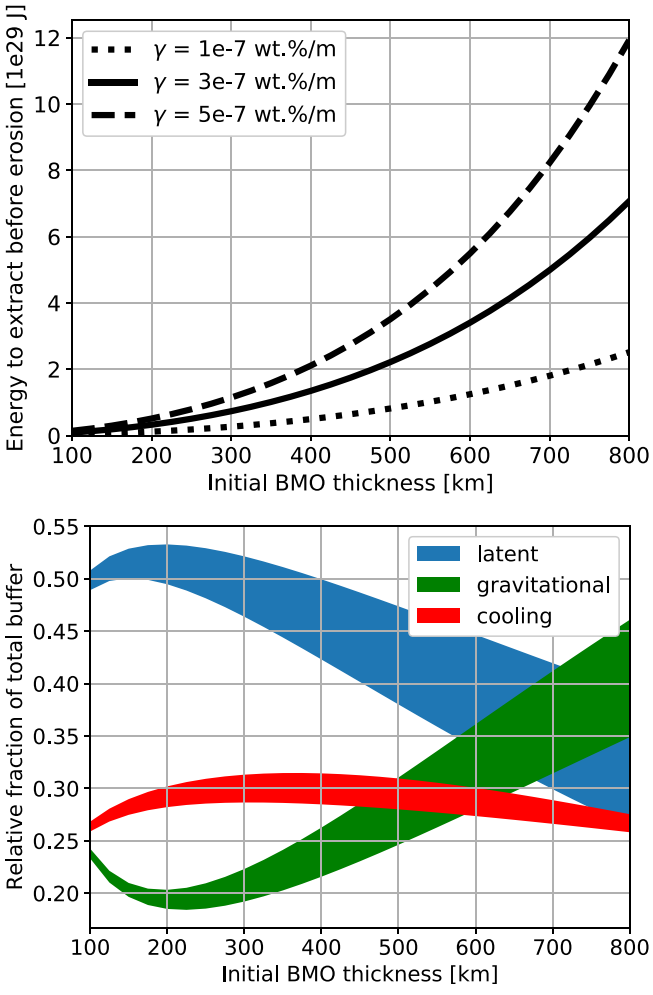

Fig. 4. (top) Size of the energy buffer added by a stratified layer of various thicknesses for different composition gradients. It includes the latent heat of crystallization, the additional cooling required by the liquidus depression due to iron enrichment at depth, and the gravitational energy required in order to mix the initial stratification. (bottom) Range of relative contribution to the global heat buffer over the range of stratification strengths 1–5 10^{-7} wt.%/m.

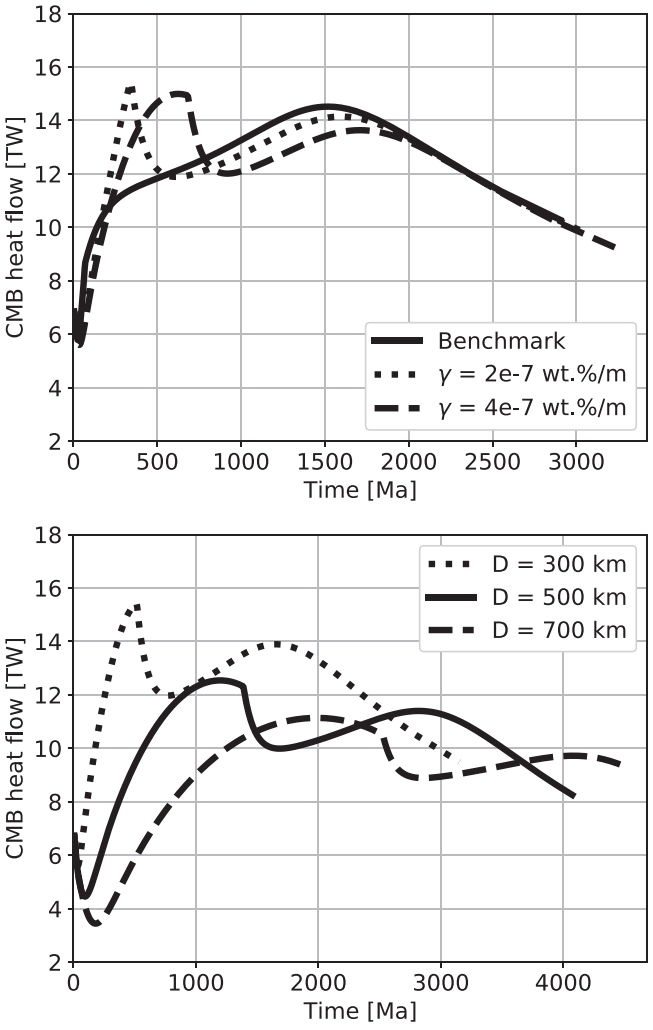

Fig. 5. Core mantle boundary heat flow as a function of time for (top) different composition gradients for D = 300 km, and (bottom) different initial layer thickness for γ = 3e-7 wt.%/m. Benchmark is a case with no initial stratification.

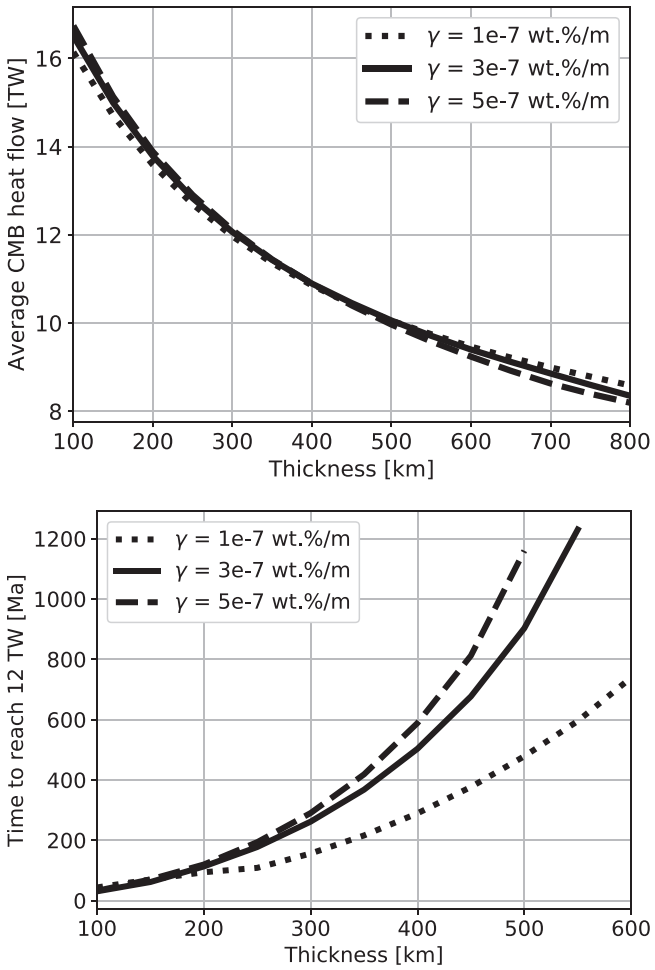

Fig. 6. (top) Average core-mantle boundary heat flow during crystallization of the basal magma ocean and (bottom), time required to reach a core-mantle boudary heat flow of 12 TW, taken here as a proxy for geodynamo onset. Values larger than that plotted on the figure never reach that threshold.

be seen in Fig. 5, top), the early low heat flow being balanced by larger values later on. The effect on the long term average is therefore minimal.

4. Discussion

The actual composition of the lower mantle being largely unknown, we chose to consider an artificial mineralogy composed of (Mg,Fe)O. The two end members have a factor two difference in density, and we take the difference in liquidus between the end-members to be 2000 K. This is justified by the fact that we do not try to predict the composition of the layer here, but to understand the general properties of the core mantle boundary heat flow as driven by a stratified layer. Early onset of the geodynamo suggests a small composition gradient and/or thin initial layer.

Compared to a well mixed magma ocean scenario, this model predicts a shutoff of the dynamo a few hundred million years after its onset, after erosion is complete. The exact timing of this shutoff cannot be predicted from these simulations, but the general structure of the evolution is characteristic of cooling driven by a stratified magma ocean. Depending on the exact amount of heat that can be extracted from the core by conduction only, our model suggests a non-continuous dynamo activity.

Contrary to the intuition, such a conductive, stratified layer does not just delay core cooling. As we have shown this is due to the liquidus depression with depth associated with the stratification. In such a system, the upper part of the layer is allowed to cool much more than a well-mixed magma ocean in the early stages of the evolution, which leads to the peak in core mantle boundary heat flow. As stratified layers may be a typical consequence of planetary formation, it is useful to understand how it couples with the other planetary layers.

For the particular case of Earth's dynamo, we have found that, though this heat buffer can save up to 100–600 K of core cooling, it is hard to maintain a thermally driven dynamo for more than a couple of billion years, depending on the appropriate value for the core heat conductivity. Low values, such as that presented in Konôpková et al. (2016) require about 3.8 ± 1.6 TW, and our model would then predict a continuous dynamo activity since its onset. On the other hand, the large values presented in, e.g., Gomi et al. (2013) require about 10 TW, which imply shutoff of the dynamo before the onset of inner core crystallization. In such a situation, an additional buoyancy source would still be required, such as MgO or SiO_2 exolution.

To summarize, the geodynamo problem is not to have enough initial potential energy in the core to sustain more than 10 TW heat flow over history (constant), it is that cores that would still leak 10 TW of heat today, would have had a much larger heat flow early in history, leading to an integrated heat loss much larger than what would be obtained from a constant 10 TW. A mechanism to keep the heat flow close to that required to sustain core convection is thus required, and a stably stratified basal magma ocean is an example of such a process. We have shown that stratification of the BMO helps sustain an "efficient" core cooling (i.e. by extracting only the amount of heat required to drive a thermal dynamo), making a long term thermal dynamo difficult, but not impossible.

Acknowledgments

ML is grateful for funding from the Itoh Foundation. SL is supported by a public grant overseen by the French National Research Agency (ANR-15-CE31-0018-01, MaCoMaOc). We wish to thank J. Rudge and an anonymous reviewer for comments that helped clarify the manuscript. The complete code and scripts to run the various simulations can be obtained by request to ML (mlaneuville@elsi.jp).

References

Andrault, D., Bolfan-Casanova, N., Lo Nigro, G., Bouhifd, M., Garbarino, G., Mezouar, M., 2011. Solidus and liquidus profiles of chondritic mantle: Implication for melting of the Earth across its history. Earth Planet. Sci. Lett. 304, 251–259.
Badro, J., Siebert, J., Nimmo, F., 2016. An early geodynamo driven by exsolution of mantle components from Earth's core. Nature 536, 326–328.
Buffett, B., 2002. Estimates of heat flow in the deep mantle based on the power requirements for the geodynamo. Geophys. Res. Lett. 29, 165–168.
Canup, R.M., 2004. Dynamics of lunar formation. Ann. Rev. Astronomy Astrophysics 42, 441–475.
Canup, R.M., 2012. Forming a Moon with an Earth-like Composition via a Giant Impact. Science 338, 1052–1055.
Cébron, D., Maubert, P., Le Bars, M., 2010. Tidal instability in a rotating and differentially heated ellipsoidal shell. Geophys. J. Int. 182, 1311–1318.
de Koker, N., Steinle-Neumann, G., Vlcek, V., 2012. Electrical resistivity and thermal conductivity of liquid Fe alloys at high P and T, and heat flux in Earth's core. Proc. Nat. Acad. Sci. U.S.A. 109, 4070–4073.
Deguen, R., Landeau, M., Olson, P., 2014. Turbulent metal–silicate mixing, fragmentation, and equilibration in magma oceans. Earth Planet. Sci. Lett. 391, 274–287.
Fischer, R., Campbell, A., Ciesla, F., 2016. Sensitivities of earth's core and mantle compositions to accretion and differentiation processes. Earth Planet. Sci. Lett. 458, 252–262.
Gomi, H., Ohta, K., Hirose, K., Labrosse, S., Caracas, R., Verstraete, M.J., Hernlund, J. W., 2013. The high conductivity of iron and thermal evolution of the Earth's core. Phys. Earth Planet. Inter. 224, 88–103.
Helffrich, G., Kaneshima, S., 2010. Outer-core compositional stratification from observed core wave speed profiles. Nature 468, 807–810.

Hernlund, J., 2016. Chemistry of core-mantle boundary. In: Terasaki, H., Fischer, R. (Eds.), Deep Earth: Physics and Chemistry of the Lower Mantle and Core. American Geophysical Union, pp. 201–208.
Hernlund, J., McNamara, A., 2014. Dynamics of the core mantle boundary region. In: Schubert, G., Bercovici, D. (Eds.), Treatise on Geophysics. second ed. Elsevier, pp. 461–519.
Hirose, K., Morard, G., Sinmyo, R., Umemoto, K., Hernlund, J., Helffrich, G., Labrosse, S., 2017. SiO_2 crystallization and compositional evolution of the Earth's core. Nature 543, 99–102.
Kimura, J., Nakagawa, T., Kurita, K., 2009. Size and compositional constraints of Ganymede's metallic core for driving an active dynamo. Icarus 202, 216–224.
Konôpková, Z., McWilliams, R.S., Gómez-Pérez, N., Goncharov, A.F., 2016. Direct measurement of thermal conductivity in solid iron at planetary core conditions. Nature 534, 99–101.
Labrosse, S., 2015. Thermal evolution of the core with a high thermal conductivity. Phys. Earth Planet. Inter. 247, 36–55.
Labrosse, S., Hernlund, J.W., Coltice, N., 2007. A crystallizing dense magma ocean at the base of the Earth's mantle. Nature 450, 866–869.
Labrosse, S., Hernlund, J.W. and Hirose, K., 2015. Fractional melting and freezing in the deep mantle and implications for the formation of a basal magma ocean. In: The Early Earth: Accretion and Differentiation (J. Badro and M.J. Walter, editors), Wiley, vol. 212 of AGU Geophysical Monograph, pp. 123–142.
Landeau, M., Olson, P., Deguen, R., Hirsh, B.H., 2016. Core merging and stratification following giant impact. Nature Geosci 9, 786–789.
Lay, T., Hernlund, J., Buffett, B.A., 2008. Core-mantle boundary heat flow. Nat. Geosci. 1, 25–32.
Le Bars, M., Cébron, D., Le Gal, P., 2015. Flows driven by libration, precession, and tides. Ann. Rev. Fluid Mech. 47, 163–193.
McDonough, W., Sun, S., 1995. The composition of the Earth. Chem. Geol. 120, 223–253.
Nomura, R., Ozawa, H., Tateno, S., Hirose, K., Hernlund, J., Muto, S., Ishii, H., Hiraoka, N., 2011. Spin crossover and iron-rich silicate melt in the Earth's deep mantle. Nature 473, 199–202.
O'Rourke, J.G., Korenaga, J., Stevenson, D.J., 2017. Thermal evolution of earth with magnesium precipitation in the core. Earth Planet Sci. Lett. 458, 263–272.
O'Rourke, J.G., Stevenson, D.J., 2016. Powering earth's dynamo with magnesium precipitation from the core. Nature 529, 387–389.
Pozzo, M., Davies, C., Gubbins, D., Alfe, D., 2012. Thermal and electrical conductivity of iron at Earth's core conditions. Nature 485, 10–15.
Sasaki, S., Nakazawa, K., 1986. Metal-silicate fractionation in the growing Earth: energy source for the terrestrial magma ocean. J. Geophys. Res. 91, 9231.
Spiegel, E.A., 1963. A generalization of the mixing-length theory of turbulent convection. Astrophys. J. 138, 216–225.
Stevenson, D.J., 2003. Planetary magnetic fields. Earth Planet. Sci. Lett. 208, 1–11.
Tateno, S., Hirose, K., Ohishi, Y., 2014. Melting experiments on peridotite to lowermost mantle conditions. J. Geophys. Res. 119, 4684–4694.
Tsuno, K., Frost, D., Rubie, D., 2013. Simultaneous partitioning of silicon and oxygen into the earth's core during early earth differentiation. Geophys. Res. Lett. 40, 66–71.
Williams, Q., Garnero, E.J., 1996. Seismic evidence for partial melt at the base of the Earth's mantle. Science 273, 1528.